JOURNAL OF SOLID STATE CHEMISTRY **121,** 332–338 (1996)
ARTICLE NO. 0045

Preparation and Transport Properties of New Ternary Tellurides $A_xNb_6Te_8$ (A = Tl, Ca, Sr, Ba, La, and Nd)

Jong-Gyu Lee, Simon Chan, K. V. Ramanujachary,[1] and Martha Greenblatt

Department of Chemistry, Rutgers, The State University of New Jersey, P.O. Box 939, Piscataway, New Jersey 08855-0939

Received August 1, 1995; in revised form October 6, 1995; accepted October 11, 1995

New ternary niobium tellurides $A_xNb_6Te_8$ (A = Ca, Sr, Ba, La, and Nd; x = 0.22–0.32) have been prepared by molten salt ion exchange reactions of $Tl_xNb_6Te_8$ with rare earth/alkaline earth iodides AI_3/AI_2 at relatively low temperatures, 535–795°C. Most of the niobium tellurides show metallic behavior followed by superconductivity at low temperatures, 4–6 K. Polycrystalline $La_{0.32}Nb_6Te_8$ and $Nd_{0.24}Nb_6Te_8$ show a resistivity anomaly at 46 and 43 K, respectively, while polycrystalline $Tl_{0.91}Nb_6Te_8$ shows a broad resistivity anomaly at 160–220 K. The resistivity anomaly observed in $Tl_{0.91}Nb_6Te_8$ appears to be accompanied by a minor structural distortion evidenced in differential scanning calorimetry. The resistivity anomalies observed in $La_{0.32}Nb_6Te_8$ and $Nd_{0.24}Nb_6Te_8$ are similar to those observed at ~40 K for Nb_3Te_4 and may be related to the onset of a charge density wave type instability.

INTRODUCTION

Recently, considerable effort has been directed toward the understanding of physicochemical properties of transition metal chalcogenides (1–6). Among many transition metal chalcogenides, both the binary and ternary niobium chalcogenides Nb_3Q_4 and $A_xNb_6Q_8$ (A = Alkali, Tl, In, etc; Q = S, Se, and Te) have attracted much interest, due to a number of interesting properties such as superconductivity, charge density wave (CDW) instabilities, and ion intercalation (7–11).

Nb_3Q_4 crystallizes in a hexagonal unit cell (space group $P6_3/m$ or $P6_3$) (7, 12). The crystal structure of Nb_3Q_4 is built up from face sharing of three NbQ_6 octahedra and by edge sharing of the resulting Nb_3Q_{11} groups (Fig. 1) (13). Each Nb atom in the NbQ_6 octahedra is displaced (by ~0.3 Å for Q = S) toward one of the faces of the octahedron, which results in the formation of infinite zigzag metal chains along the c axis (12). The shortest Nb–Nb intrachain distances are 2.88(1), 2.80(1), and 2.97(1) Å for Q = S, Se, and Te, respectively, which are comparable to those in metallic Nb(d_{Nb-Nb} = 2.86 Å). On the other hand, the interchain Nb–Nb distances between face-shared octahedra are considerably longer, 3.37(1), 3.47(1), and 3.65(1) Å, respectively, suggesting a quasi-one-dimensional nature of the electronic structure. Another important structural feature of the Nb_3Te_4-type compounds is the hexagonal tunnels running along the c axis. The empty tunnels in Nb_3Q_4 are large enough to accommodate ions in the voids.

Nb_3S_4, Nb_3Se_4, and Nb_3Te_4 exhibit metallic conductivity ($\rho_{RT} = 10^{-3}$–10^{-4} $\Omega \cdot$cm) as well as a superconducting transition at 4.0, 2.0, and 1.8 K, respectively (8). Ishihara and Nakada observed two types of phase transitions in a Nb_3Te_4 single crystal at ~20 and ~80 K from resistivity and thermoelectric power measurements (14–16). Surzuki *et al.* subsequently showed that the transition at ~80 K in Nb_3Te_4 is associated with CDW formation (17–18). In 1987, Sekine *et al.* also observed two anomalies at 40 and 110 K in both the resistivity and the magnetic susceptibility data, where the 110 K phase transition is accompanied by the appearance of superlattice reflections which are characterized by commensurate wave vectors $\mathbf{q} = \pm(\frac{1}{3}\mathbf{a}^* + \frac{1}{3}\mathbf{b}^*) + \frac{3}{7}\mathbf{c}^*$ (19).

Calculations of the electronic band structures of Nb_3Q_4 by several groups indicate a quasi-one-dimensional character of these phases (9, 20, 21). The Fermi level of Nb_3S_4 lies below a minimum of the density of states (DOS) curve. However, the position of the Fermi level can be altered by addition/removal of electrons in the Nb_3S_4 structure.

The first ternary niobium chalcogenides $A_xNb_6S_8$ (A = Li, Na, K, Ca) were prepared both (i) electrochemically and (ii) by solid state reaction by Schölhorn and Schramm (22). They found that the superconducting transition of Nb_3S_4 increased: T_c = 7.3 K for $K_{0.4}Nb_6S_8$.

Huan and Greenblatt subsequently prepared many isotypic compounds by means of molten salt ion exchange or ternary element insertion methods: $A_xNb_6S_8$ (A = Na, K, Rb, Tl, Cu, Ag, Zn, Pb, and Bi; $0.67 \le x \le 1.0$), $A_xNb_6Se_8$ (A = Tl, Sn, Pb, and Bi; $0.4 \le x \le 1.0$), and $A_xNb_6Te_8$ (A = Na, K, Rb, Cs, Tl, Cu, Ag, In, Zn, Cd, Sn, Pb, and Bi; $0.67 \le x \le 2.0$) (10, 23). They also observed a

[1] Current address: Chemistry Department, Rowan College of New Jersey, Glassboro, NJ 08028-1701.

0022-4596/96 $18.00

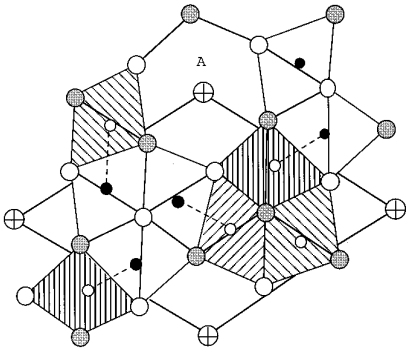

FIG. 1. Structure of $A_xNb_6O_8$ (Q = S, Se, Te; A = alkali, alkaline earth, Tl, etc.). Shaded and unshaded octahedra are on level $z = \frac{1}{4}$ and $z = \frac{3}{4}$, respectively.

considerable increase in T_c with the insertion of ternary elements into the empty tunnels of Nb_3Q_4: for example, T_c = 4.3, 5.8, and 6.3 K for A = Tl, Bi, and Pb in $A_xNb_6Te_8$ (24).

Recently, Ohtani *et al.* have prepared $In_xNb_3Q_4$ ($0 \leq x$ 1.0; Q = S, Se, Te) by the ternary element insertion method (11). All the polycrystalline samples show metallic behavior in the temperature range 1.5–273 K, with an anomalous jump of resistivity at 40–140 K for tellurides with x = 0.10–1.0. Electron diffraction measurements showed the 140 K transition to be associated with a CDW formation evidenced by the appearance of a superstructure with the commensurate wave vectors $q = \pm(\frac{1}{3}\mathbf{a}^* + \frac{1}{3}\mathbf{b}^*) + \frac{4}{9}\mathbf{c}^*$.

Since the first report of ternary niobium chalcogenides $A_xNb_6S_8$ (A = Li, Na, K, and Ca) by Schölhorn and Schramm, there have been many isotypic compounds prepared. However, alkaline earth (M^{2+}) and rare earth (Ln^{3+}) cations in $A_xNb_6Te_8$ have not been investigated systematically (10, 23). As already predicted both from theoretical calculations and experimental results, it is feasible to insert both di- and trivalent ions into the empty channels of Nb_3Te_4-type compounds (9). In the present paper, we report some new ternary niobium chalcogenides of the type $A_xNb_6Te_8$, where A = Ca, Sr, Ba, La, Nd, and Tl, and their electrical and magnetic properties.

SYNTHESIS

Preparation of $Tl_xNb_6Te_8$ by Solid State Method

The ternary $Tl_xNb_6Te_8$ phases were prepared according to the procedure reported earlier (10, 23). First, TlTe were prepared by heating pellets of a stoichiometric mixture of elemental Tl (Aldrich, 99.999%) and Te (Alfa, 99.99%) in a sealed quartz tube at 450°C for 4 h. Next, stoichiometric amounts of (TlTe + 6 Nb + 7 Te) were mixed and pressed into pellets. The pellets were placed in a quartz tube, which was subsequently sealed under high vacuum, $\sim 10^{-6}$ Torr, and heated at 1000°C for 10 days.

Preparation of $A_xNb_6Te_8$ (A = Ca, Sr, Ba, La, and Nd) by Molten Salt Ion Exchange Reaction

The molten salt ion exchange reactions were carried out according to the equation

$$Tl_xNb_6Te_8 + y\,AI_3/AI_2 \rightarrow A_zNb_6Te_8 + x\,TlI + \text{excess } AI_3/AI_2.$$

The powdered mixture of either $Tl_xNb_6Te_8$ and $y\,AI_3$ (LaI_3, 99.9%; NdI_3, 99.99%; Alfa; y = 1.5–2) or $Tl_xNb_6Te_8$ and 2 AI_2 (CaI_2, 99.999%; SrI_2, 99.998%; BaI_2, 99.999%; Alfa) was mixed and pressed into a pellet under helium atmosphere and sealed in a quartz tube under high vacuum, $\sim 10^{-6}$ Torr. The sealed quartz tube was placed in a horizontal tube furnace with one end close to room temperature. Initially, the temperature of the sample in the hot zone was increased up to 450°C and held for 3–4 days. The set temperature 450°C is ~10°C higher than the melting point of TlI. The tube was then heated at the final reaction temperatures, 804, 535, 760, 790, and 795°C for Ca, Sr, Ba, La, and Nd, respectively, which are approximately ~10–20°C higher than the melting point of corresponding iodides, AI_3 or AI_2.

CHARACTERIZATION

X-ray powder diffraction patterns of all the samples were recorded with a SCINTAG PAD V diffractometer with Cu$K\alpha$ radiation in the 2θ range 5°–65°. Si or W powders were used as internal standards and cell parameters were obtained from least-square refinement of the observed d spacings.

The dc electrical resistivities were measured on brick-shaped polycrystalline pellet with a DE 202 cryostat (APD Cryogenics) by a four-probe method between 25 and 300 K. Ohmic contacts were made either by attaching molten indium ultrasonically to the four spots of conducting silver paste on the sides of the specimens or by anchoring thin copper wires (diameter ~0.04 mm) on the sides of the specimens with a conductive Ag paint.

The magnetic susceptibility of the samples was measured in a SQUID magnetometer (Quantum Design) in the temperature range 2 ~ 300 K at applied magnetic fields 25 ~ 1000 G. Brick shaped specimens, similar to those used for the resistivity measurements, were employed in the magnetic property investigations.

TABLE 1
Unit Cell Parameters of $A_xNb_6Te_8$ (A = Na, Tl, La, and Nd) Phases

Compound	a (Å)	c (Å)	c/a	V (Å^3)
Nb_3Te_4[a]	10.671(1)	3.6468(1)	0.3418	359.6(1)
$Na_{0.86}Nb_6Te_8$[b]	10.653(1)	3.642(2)	0.3419	357.8(1)
$Zn_{1.0}Nb_6Te_8$[b]	10.651(1)	3.639(1)	0.3437	357.5(1)
$Bi_{0.67}Nb_6Te_8$[b]	10.648(1)	3.636(1)	0.3415	357.0(1)
$Tl_{0.91}Nb_6Te_8$	10.673(1)	3.652(1)	0.3422	360.3(1)
$La_{0.32}Nb_6Te_8$	10.680(1)	3.637(1)	0.3405	359.3(1)
$Nd_{0.24}Nb_6Te_8$	10.672(1)	3.647(2)	0.3417	359.7(2)
$Ca_xNb_6Te_8$	10.670(1)	3.647(1)	0.3418	359.6(1)
$Sr_{0.22}Nb_6Te_8$	10.699(1)	3.630(1)	0.3393	359.9(1)
$Ba_{0.24}Nb_6Te_8$	10.668(2)	3.649(2)	0.3421	359.6(1)

Note. Space group = $P6_3/m$. Internal standard = W.
[a] Calculated from a and c in Ref. (7).
[b] Calculated from a and c in Ref. (24).

A microprocessor-controlled dc plasma atomic emission spectrometer (Spectrametrics, Inc., SMI III) was used for the composition analysis of the samples.

RESULTS AND DISCUSSION

Table 1 lists the unit cell parameters of pure $Tl_xNb_6Te_8$ and of the new $A_xNb_6Te_8$ (A = Ca, Sr, Ba, La, and Nd) phases. Polycrystalline $Tl_xNb_6Te_8$ and $A_xNb_6Te_8$ were prepared by solid state reactions and by molten salt ion exchange reactions, respectively. All the ternary niobium chalcogenides were synthesized in the pure form. However, powder X-ray diffraction patterns of new $La_xNb_6Te_8$ and $Nd_xNb_6Te_8$ sometimes show additional weak peaks at ~8.8°, 36.3°, and 50.2°, probably due to either lowering of symmetry or an unknown impurity phase. The unit cell parameters of all new tellurides (A = Ca, Sr, Ba, La, and Nd) were similar to those of the binary Nb_3Te_4 and the starting compound $Tl_{0.91}Nb_6Te_8$, suggesting that the unit cell parameters were not affected by the size of the A ions. However, this is not surprising because the Nb_3Te_4 structure has a rigid skeleton due to the stable Nb–Nb and Nb–Te bonds. Similar results were observed in many other ternary chalcogenides (10, 11, 23). The observed and calculated d spacings of $A_xNb_6Te_8$ are compared in Table 2.

Plasma atomic emission (PAE) measurements showed that the x values are 0.91, 0.32, 0.24, 0.24, and 0.22, for Tl, La, Nd, Ba, and Sr, respectively within an experimental error ~10%. We could not determine the Ca content in $Ca_xNb_6Te_8$ samples due to a precipitation in the solution. The PAE also confirmed that no Tl remained in the powdered samples after the ion exchange reaction of $Tl_xNb_6Te_8$ by La, Nd, Ba, Sr, and Ca, indicating no mixed occupancy at the A site in $A_xNb_6Te_8$ compositions.

The temperature dependence of the electrical resistivities of $A_xNb_6Te_8$ in the range 25–300 K are shown in Figs. 2 and 3. All the samples show metallic behavior over the entire temperature range of measurement with anomalous increases of resistivity at low temperature. $Tl_{0.91}Nb_6Te_8$ shows a broad transition at 160–220 K (Fig. 2a). This transition was also observed in differential scanning calorimetric analysis, where a small endothermic peak was observed at 163 K, suggesting a possible minor structural distortion. The resistivity anomaly at 160–220 K might be due to a CDW-type instability. Magnetic susceptibility measurements of $Tl_{0.91}Nb_6Te_8$ indicate typical Pauli paramagnetism in the temperature range 2–300 K and show no evidence of superconductivity down to 2 K. This is in contrast to Huan *et al.*'s observation of a superconducting transition at 4.3 K for $TlNb_6Te_8$ by electrical resistivity measurement (24). Presently, it is not clear why the $Tl_{0.91}Nb_6Te_8$ samples studied here are not superconducting. It is possible that the superconductivity is suppressed by a CDW formation in our $Tl_{0.91}Nb_6Te_8$ samples, since the density of states near the Fermi level decrease with a CDW formation. The absence of superconductivity in the $Tl_{0.91}Nb_6Te_8$ samples might be explained in terms of the competition between superconductivity and CDW instabilities.

$La_{0.32}Nb_6Te_8$ (Fig. 2b) and $Nd_{0.24}Nb_6Te_8$ (Fig. 2c) show metallic behavior in the temperature range 25–300 K, with an anomalous transition at 46 and 43 K, respectively. A very small hysteresis was observed upon heating and cooling for both compounds. These transitions in the A = La and Nd phases are most likely due to CDW instabilities, similar to that observed in Nb_3Te_4 single crystals by Sekine *et al.* (19). They observed an anomaly at ~40 K both in the resistivity and magnetic susceptibility, although superlattice lines in the electron diffraction patterns were not observed below 40 K in Nb_3Te_4. Both $La_{0.32}Nb_6Te_8$ and $Nd_{0.24}Nb_6Te_8$ show an unusual nonlinear behavior of electrical resistivity with a positive curvature in the range 25–300 K. The resistivity near room temperature decreases slowly, while at low temperature it decreases rapidly with decreasing temperature. This broad deviation of resistivity from linearity could be due to disorder of the A cations in the tunnels.

$Ca_xNb_6Te_8$, $Sr_{0.22}Nb_6Te_8$, and $Ba_{0.24}Nb_6Te_8$ also show metallic behavior in the temperature range 25–300 K (Fig. 3). These compounds do not show any resistivity anomaly down to 30 K except a broad positive curvature, which is similar to that observed in $La_{0.32}Nb_6Te_8$.

The magnetic susceptibility of $La_{0.32}Nb_6Te_8$ (Fig. 4) revealed a sharp superconducting transition (T_c^{onset} = 4 K) and $Ca_xNb_6Te_8$, $Sr_{0.22}Nb_6Te_8$, and $Ba_{0.24}Nb_6Te_8$ showed a broad superconducting transition (T_c^{onset} = 6 K) with typical Pauli-paramagnetic behavior above these transition temperatures (Figs. 4 and 5). The T_c's observed at 4–6 K for $A_xNb_6Te_8$ (A = Ca, Sr, Ba, and La) are significantly higher than that of Nb_3Te_4 at 1.8 K. However, $Nd_{0.24}Nb_6Te_8$

TABLE 2
Powder X-Ray Diffraction Data of $A_xNb_6Te_8$ Phases (A = Tl, La, Nd, Ca, Sr, and Ba)

	$Tl_{0.91}Nb_6Te_8$			$La_{0.32}Nb_6Te_8$			$Nd_{0.24}Nb_6Te_8$		
hkl	d_{obs} (Å)	d_{calc} (Å)	I/I_o	d_{obs} (Å)	d_{calc} (Å)	I/I_o	d_{obs} (Å)	d_{calc} (Å)	I/I_o
100	9.26	9.24	42	9.27	9.26	89	9.24	9.24	78
110	5.338	5.337	7	5.342	5.345	10	5.338	5.336	11
210	3.494	3.494	3	3.499	3.499	4	3.490	3.493	7
300	3.081	3.081	72	3.087	3.086	72	3.081	3.081	61
111	3.014	3.014	7	3.009	3.007	6	3.014	3.011	2
201		2.865		2.859	2.860	20	2.863	2.863	6
310	2.564	2.564	99	2.568	2.568	99	2.565	2.563	99
211	2.524	2.525	23	2.522	2.522	42	2.523	2.523	20
301		2.355		2.353	2.353	5		2.353	
400	2.310	2.311	2		2.314		2.311	2.311	5
221	2.154	2.155	11	2.154	2.154	19	2.154	2.153	9
320	2.120	1.121	10	2.123	2.124	10	2.120	2.120	12
311	2.099	2.098	7	2.098	2.098	12	2.096	2.097	4
410	2.017	2.017	20	2.020	2.020	19	2.017	2.017	20
500	1.849	1.849	13	1.851	1.852	16	1.848	1.849	21
321		1.834		1.834	1.834	16	1.835	1.833	9
420	1.746	1.747	11	1.749	1.750	15	1.746	1.747	13
510	1.660	1.660	5		1.663		1.659	1.660	6
501		1.649		1.650	1.650	9	1.648	1.649	5
331		1.599		1.600	1.600	5	1.598	1.599	4
430	1.520	1.520	2		1.522			1.520	
312		1.487			1.484		1.485	1.486	4
520		1.480		1.482	1.482	12	1.479	1.480	9

	$Ca_xNb_6Te_8$			$Sr_{0.22}Nb_6Te_8$			$Ba_{0.24}Nb_6Te_8$		
hkl	d_{obs} (Å)	d_{calc} (Å)	I/I_o	d_{obs} (Å)	d_{calc} (Å)	I/I_o	d_{obs} (Å)	d_{calc} (Å)	I/I_o
100	9.245	9.241	73	9.274	9.266	58	9.256	9.239	58
110	5.335	5.335	12	5.341	5.350	9	5.341	5.334	11
210		3.493			3.502			3.492	
300	3.081	3.080	70	3.089	3.089	62	3.081	3.080	43
111	3.010	3.011	6	3.002	3.004	15	3.013	3.012	22
201	3.862	3.862	15	2.858	2.858	48	2.864	2.863	54
310	2.563	2.563	99	2.570	2.570	99	2.564	2.562	99
211	2.523	2.522	22	2.521	2.520	89	2.523	2.523	89
301		2.353		2.351	2.352	13		2.354	
400	2.310	2.310	8		2.316			2.310	
221	2.154	2.153	12	2.154	2.153	41	2.154	2.153	40
320		2.120			2.126			2.120	
311	2.096	2.097	8	2.098	2.098	27	2.097	2.097	23
410	2.016	2.016	32	2.021	2.022	26	2.014	2.016	25
500	1.848	1.848	28	1.853	1.853	18	1.848	1.848	17
321	1.833	1.833	12	1.835	1.834	34	1.833	1.833	36
420	1.746	1.746	19	1.751	1.751	19	1.744	1.746	14
510		1.660			1.664			1.659	
501	1.649	1.649	9	1.650	1.651	22	1.648	1.649	24
331	1.598	1.598	4	1.602	1.601	10	1.598	1.598	12
430		1.519			1.523			1.519	
312		1.486		1.482	1.483	23		1.486	
520	1.479	1.480	9		1.484			1.480	

Note. Space group = $P6_3/m$. Internal standard = W powder.

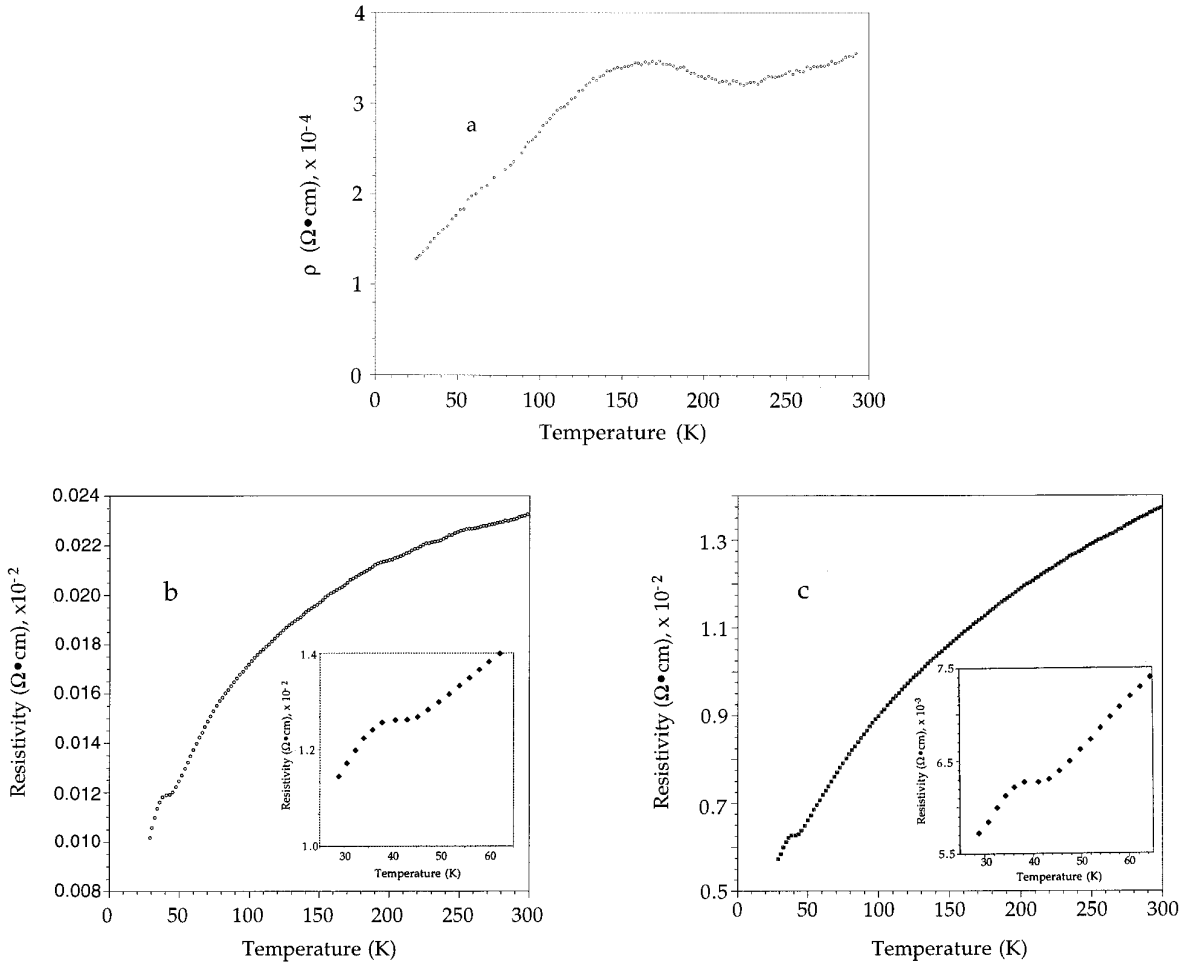

FIG. 2. Temperature dependence of electrical resistivity of (a) $Tl_{0.91}Nb_6Te_8$, (b) $La_{0.32}Nb_6Te_8$, and (c) $Nd_{0.24}Nb_6Te_8$. There is a broad resistivity anomaly at 160–220 K for $Tl_{0.91}Nb_6Te_8$ and a resistivity anomaly at 46 and 43 K for $La_{0.32}Nb_6Te_8$ and $Nd_{0.24}Nb_6Te_8$, respectively.

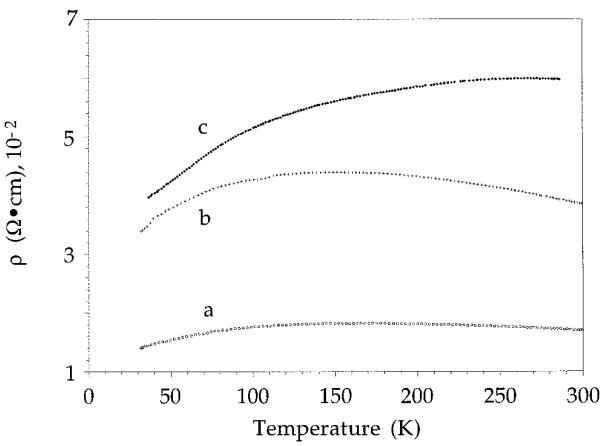

FIG. 3. Temperature dependence of electrical resistivity of (a) $Ca_xNb_6Te_8$, (b) $Sr_{0.22}Nb_6Te_8$, and (c) $Ba_{0.24}Nb_6Te_8$.

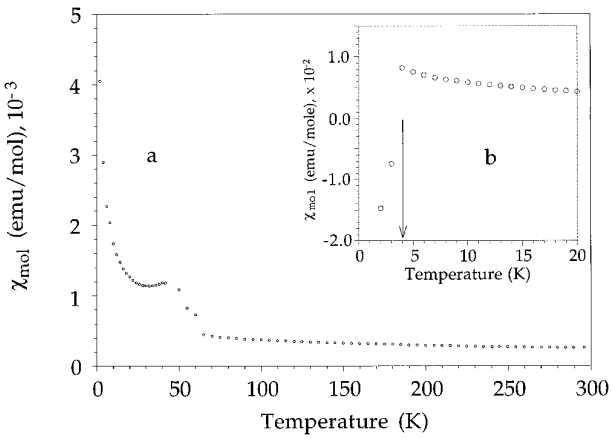

FIG. 4. Magnetic susceptibility of $La_{0.32}Nb_6Te_8$ in the temperature range 2–300 K. The inset shows a sharp superconducting transition at 4 K (T_c^{onset}).

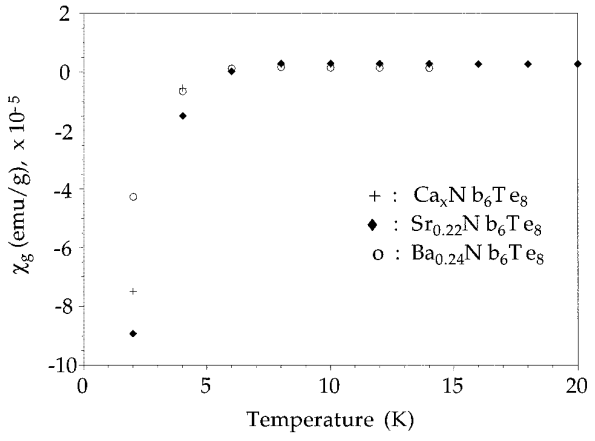

FIG. 5. Magnetic susceptibility measurements of $Ca_xNb_6Te_8$, $Sr_{0.22}Nb_6Te_8$, and $Ba_{0.24}Nb_6Te_8$ in the temperature range 2–300 K. All show a superconducting transition at ~6 K (T_c^{onset}).

did not show any evidence of superconductivity down to 2 K. The absence of superconductivity in $Nd_{0.24}Nb_6Te_8$ may be attributed to the highly paramagnetic Nd^{3+} ions in $Nd_{0.24}Nb_6Te_8$ (Fig. 6). The inset shows a slower increase of susceptibility at ~3 K, probably due to either the onset of a short-range antiferromagnetic correlation between the Nd^{3+} moments, or the formation of a filamentary superconducting state. Detailed ac susceptibility and electrical resistivity measurements below 4 K would be needed to further clarify this anomaly. Provided that the temperature-independent magnetic susceptibility (χ_o) is negligible as seen in $La_{0.32}Nb_6Te_8$, the Curie ($C = 0.87$ mole/emu · K) and Weiss ($\theta = 28$ K) constants were obtained by analyzing the susceptibility data in the temperature range 200–300 K, following a modified Curie–Weiss equation,

$$\chi = \chi_p + C/(T - \theta),$$

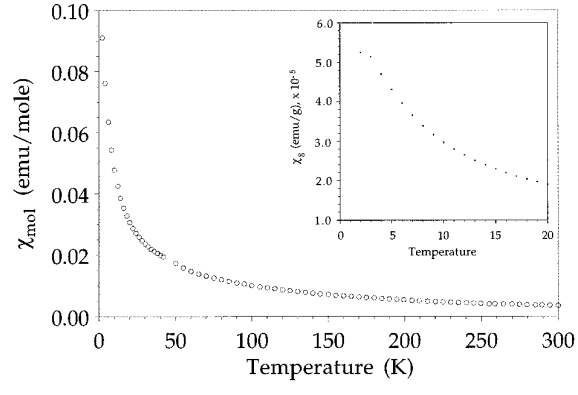

FIG. 6. Magnetic susceptibility of $Nd_{0.24}Nb_6Te_8$ in the temperature range 2–300 K. The inset shows a slower increase of susceptibility at ~3 K, probably due to either a short-range antiferromagnetic coupling or a formation of filamentary superconducting state.

where χ_p is the Pauli susceptibility due to conduction electrons. Pauli susceptibility was estimated based on the temperature-independent susceptibility (100–300 K) observed for $La_{0.32}Nb_6Te_8$ (Fig. 4). The effective magnetic moment ($\mu_B = 2.63$) would correspond to $x = 0.51$ in $Nd_xNb_6Te_8$, assuming spin-only contribution of $4f^3$ electrons, which is somewhat higher than the value estimated from PAE analysis ($x = 0.24$). However, strong covalent interactions between Nd and Te might be responsible for the observed magnetic data.

CONCLUSION

The ternary niobium chalcogenides, $A_xNb_6Te_8$ (A = Ca, Sr, Ba, La, and Nd) were prepared by molten salt ion exchange reactions of $Tl_{0.91}Nb_6Te_8$ and the corresponding iodides (CaI_2, SrI_2, BaI_2, LaI_3, and NdI_3) at low temperatures, 535–795°C. $La_{0.32}Nb_6Te_8$, $Ca_xNb_6Te_8$, $Sr_{0.22}Nb_6Te_8$, and $Ba_{0.24}Nb_6Te_8$ show a superconducting transition at 4–6 K, while $Tl_{0.91}Nb_6Te_8$ and $Nd_{0.24}Nb_6Te_8$ do not show any evidence of diamagnetism down to 2 K. $Tl_{0.91}Nb_6Te_8$ shows a broad resistivity anomaly at 160–220 K, which is also evidenced by DSC analysis. Both $La_{0.32}Nb_6Te_8$ and $Nd_{0.24}Nb_6Te_8$ exhibit an anomaly in the temperature dependence of resistivity at ~46 and ~43 K, respectively, which suggest a CDW instability similar to that observed in Nb_3Te_4 single crystals at ~40 K.

ACKNOWLEDGMENTS

We thank Dr. Guohe Huan for helpful discussions for the preparation of the samples. This work was supported by NSF Solid State Chemistry Grants DMR-91-19301 and DMR-93-14605.

REFERENCES

1. C. N. R. Rao and K. P. R. Pisharody, *Prog. Solid State Chem.* **10**(4), 207 (1976).
2. F. J. DiSalvo, *Ferroelectrics* **17,** 361 (1977).
3. H. F. Franzen, *Prog. Solid State Chem.* **12,** 1 (1978).
4. F. J. DiSalvo, *Science* **247,** 649 (1990).
5. M. G. Kanatzidis, *Chem. Mater.* **2,** 353 (1990).
6. P. M. Keane, Y.-J. Lu, and J. A. Ibers, *Acc. Chem. Res.* **24,** 223 (1991).
7. K. Selte and A. Kjekshus, *Acta Crystallogr.* **17,** 1568 (1964).
8. E. Amberger, K. Polhorn, P. Grimm, M. Dietrich, and B. Obst, *Solid State Commun.* **26,** 943 (1978).
9. E. Canadell and M.-H. Whangbo, *Inorg. Chem.* **25,** 1488 (1986).
10. G. Huan and M. Greenblatt, *Mater. Res. Bull.* **22,** 943 (1987).
11. T. Ohtani, Y. Sano, and Y. Yokota, *J. Solid State Chem.* **103,** 504 (1993).
12. A. F. Ruysink, F. Kadijk, A. J. Wagner, and F. Jellinek, *Acta Crystallogr. Sect. B* **24,** 1614 (1968).
13. M. Vlasse and L. Fournes, *Mater. Res. Bull.* **11,** 1527 (1976).
14. Y. Ishihara and I. Nakada, *Solid State Commun.* **44**(10), 1439 (1982).
15. Y. Ishihara and I. Nakada, *Solid State Commun.* **42**(8), 579 (1982).
16. Y. Ishihara and I. Nakada, *Solid State Commun.* **45**(2), 129 (1983).
17. K. Suzuki, M. Ichihara, I. Nakada, and Y. Ishihara, *Solid State Commun.* **52**(8), 743 (1984).

18. K. Suzuki, M. Ichihara, I. Nakada, and Y. Ishihara, *Solid State Commun.* **59**(5), 291 (1986).
19. T. Sekine, Y. Kiuchi, E. Matsura, K. Uchinokura, and R. Yoshizaki, *Phys. Rev. B* **36,** 3153 (1987).
20. D. W. Bullett, *J. Solid State Chem.* **33,** 13 (1980).
21. A. Oshiyama, *Jpn. J. Phys. Soc.* **53**(2), 587 (1983).
22. R. Schölhorn and W. Schramm, *Z. Naturforsch. B* **34,** 697 (1979).
23. G. Huan and M. Greenblatt, *Mater. Res. Bull.* **22,** 505 (1987).
24. G. Huan, Ph.D. Thesis, Rutgers University, 1989.